the estimates $e_\sigma(z) = \sim 970\ cm^{-1}$ and $e_\pi(z) = \sim 162.5\ cm^{-1}$ for the axial ligands in $(cyclamH_4)CuCl_6$. However, it has been suggested that a dependence of this kind probably overestimates the bonding interactions of distant ligands[48] and that their effects may be better approximated by assuming that the bonding parameters are proportional to the square of the metal–ligand diatomic overlap integrals. The relevant overlap integrals have been estimated[49] as ~0.076 and ~0.025 ($\sigma$ overlaps) and ~0.035 and ~0.009 ($\pi$ overlaps) at 229 and 317.5 pm, respectively, implying the values $e_\sigma(z) = \sim 530\ cm^{-1}$ and $e_\pi(z) = \sim 55\ cm^{-1}$ for the axial ligands. Taking both these approaches into consideration, the very approximate estimates $e_\sigma(z) = \sim 700\ cm^{-1}$ and $e_\pi(z) = \sim 75\ cm^{-1}$ may be made for the axial chlorides in $(cyclamH_4)CuCl_6$. Substitution into eq 1b yields the value $e_{ds} \simeq 1175\ cm^{-1}$ for the $CuCl_6^{4-}$ ion in this complex.

The parameter $e_{ds}$ describes the energy by which the $^2A_{1g}(z^2)$ state is depressed by d–s mixing, this being $4e_{ds}$.[9] Simple perturbation theory implies that the fractional occupancy of the 4s orbital in this state is $4e_{ds}/E_{4s}$. Here, $E_{4s}$ is the energy separation between the 3d and 4s orbitals, which may be estimated[50] as $\sim 80\,000\ cm^{-1}$. These values thus imply ~5.8% occupancy of the 4s orbital in the $^2A_{1g}(z^2)$ state of $(cyclamH_4)CuCl_6$. This is somewhat less than the value of ~7.6% obtained from the above average data of the planar $CuCl_4^{2-}$ ion, which is as expected, since the degree of mixing depends upon the difference between the interaction of the ligands in the $xy$ plane and along the $z$ axis.[40] These estimates may be compared with those obtained from the analysis of the metal hyperfine parameters derived from the EPR spectra of copper(II) complexes having $^2A_{1g}(z^2)$ ground states. It has been deduced[51] that the unpaired electron spends ~3.2% of its time in the metal 4s orbital in the compressed tetragonal complex $CuF_6^{4-}$, which compares quite favorably with the above estimate of ~5.8% for the $CuCl_6^{4-}$ ion when it is remembered that the fluoro complex departs much less from a regular octahedral geometry[52] than is the case for the chloro complex. In the linear $CuF_2$ molecule, which is the limiting complex formed by tetragonally compressing an octahedral copper(II) complex, the 4s occupancy apparently rises to ~33% in the ground state.[51,53] This very high value presumably results from the extremely short Cu–F bonds, which means that the ligand-field anisotropy is much greater than in the limiting complex formed by axial elongation, planar $CuCl_4^{2-}$. The general self-consistency of this picture is confirmed by a recent analysis of the "d–d" spectrum of the linear $NiO_2^{2-}$ ion,[54] which implied ~25% contribution of the 4s orbital to the $a_{1g}(z^2)$ orbital.

**Acknowledgment.** Professor Th. A. Kaden of the Chemistry Department of the University of Basel is thanked for a gift of the crystals of $(cyclamH_4)CuCl_6$ and for providing details of the crystal structure of the complex prior to publication. The receipt of a Humboldt Research Fellowship by M.A.H. for the period when much of the work was undertaken and a University of Tasmania postgraduate award to R.G.M. are gratefully acknowledged, as is financial assistance from the Australian Research Grants Scheme.

**Registry No.** $(cyclamH_4)CuCl_6$, 122648-03-7.

(48) Smith, D. W. *J. Chem. Soc. A* **1971**, 1024.
(49) Smith, D. W. *J. Chem. Soc. A* **1970**, 1498.
(50) An upper limit of $\sim 100\,000\ cm^{-1}$ is placed on this energy by the photoelectron spectra of various copper(II) complexes. See: Jørgensen, C. K. *Struct. Bonding (Berlin)* **1975**, *24*, 28.
(51) Hitchman, M. A.; McDonald, R. G.; Reinen, D. *Inorg. Chem.* **1986**, *25*, 519.
(52) The Jahn–Teller radius of $CuF_6^{4-}$ is about 36.5 pm: Reinen, D.; Krause, S. *Inorg. Chem.* **1981**, *20*, 2750.
(53) Kasai, P. H.; Whipple, E. B.; Weltner, W. *J. Chem. Phys.* **1966**, *44*, 2581.
(54) Hitchman, M. A.; Stratemeier, H.; Hoppe, R. *Inorg. Chem.* **1988**, *27*, 2506.

Contribution from the Chemistry Department, University of Virginia, Charlottesville, Virginia 22901

# Infrared Spectra of $As_4$–Ozone Reaction and Photolysis Products in Solid Argon

Lester Andrews* and Zofia Mielke†

*Received April 26, 1988*

$As_4$ and $O_3$ codeposited with excess argon at 14–17 K produced new sharp weak bands at 921.7, 590.3, and 565.4 $cm^{-1}$ that increased with red-light photolysis. In the early stages of 630–1000-nm irradiation, the upper band was favored, but in later stages the upper band decreased while the lower bands increased. These single O atom species are assigned to AsO complex and bridge-bonded $As_4O$ formed by decomposition of excited terminally bound $As_4O$. New bands in the 700–810-$cm^{-1}$ region below $As_4O_6$ that were favored on UV photolysis are assigned to bridge-bonded $As_4O_x$ ($x$ = 2–5) species; $As_4O_6$ was also formed on codeposition and increased by UV photolysis. $As_4$ is more reactive with $O_3$ than $P_4$ under the conditions of these experiments.

## Introduction

Although spectroscopy of the smallest arsenic oxide, AsO, and the largest arsenic oxides, $As_4O_6$ and $As_4O_{10}$, have been extensive,[1-6] there has been no characterization of smaller intermediate arsenic oxide species. However, the larger $As_4O_x$ ($x$ = 6–10) species evaporating from the solid oxides have been examined by matrix infrared methods.[7] Several new lower oxides of phosphorus have been identified and characterized in this laboratory from matrix reactions of $P_4$ with oxygen atoms,[8] and this approach has been applied to the arsenic–oxygen system. The tetrahedral $As_4$ vapor species has been characterized,[9-12] and the controlled reaction of $As_4$ with O atoms is the subject of this matrix investigation.

† On leave from the Institute of Chemistry, Wroclaw University, Wroclaw, Poland.

(1) Anderson, V. M.; Callomon, J. H. *J. Phys. B* **1973**, *6*, 1664.
(2) Uehara, H. *Chem. Phys. Lett.* **1981**, *84*, 539.
(3) Beattie, I. R.; Livingstone, K. M. S.; Ozin, G. A.; Reynolds, D. J. *J. Chem. Soc. A* **1970**, 449.
(4) Brumbach, S. B.; Rosenblatt, G. M. *J. Chem. Phys.* **1972**, *56*, 3110.
(5) Rytter, E.; Goates, S. K.; Papatheodorou, G. N. *J. Chem. Phys.* **1978**, *69*, 3717.
(6) Szymanski, H. A.; Marabella, L.; Hoke, J.; Harter, J. *Appl. Spectrosc.* **1968**, *22*, 297.
(7) Brisdon, A. K.; Gomme, R. A.; Odgen, J. S. *J. Chem. Soc., Dalton Trans.* **1986**, 2725.
(8) (a) Andrews, L.; Withnall, R. *J. Am. Chem. Soc.* **1988**, *110*, 5605. (b) Andrews, L.; Mielke, Z. To be submitted for publication. The photosensitive 1197-$cm^{-1}$ band is probably due to a $(P_3)(PO)$ complex.

0020-1669/89/1328-4001$01.50/0 

**Table I.** Product Absorptions ($cm^{-1}$) Observed in $As_4$ Codeposition Experiments with Ozone in Excess Argon at 12 K

| | band photolysis behavior[a] | | | | | | |
|---|---|---|---|---|---|---|---|
| $As_4 + {}^{16}O_3$ | 630(I) nm | 630(II) nm | 470 nm | 380 nm | 290 nm | $As_4 + {}^{18}O_3$ | ident[b] |
| 1096 | d | | | | | 1035 | $As_4$---$O_3$ |
| 1034 | d | | | | | 977 | $As_4$---$O_3$ |
| 981.5 | | i | i | i | c | 935.5 | $As_4O$ (**3**) |
| 961 | | | | i | i | 917 | X---AsO (**4**) |
| 952.0 | i | i | i | d | d | 908.0 | X---AsO (**4**) |
| 921.7 | i | i | d | | | 878.8 | $(As_3)(AsO)$ (**1**) |
| 831 | i | i | i | i | i | 790.5 | $As_4O_6$ (m) |
| 805 | | | | i | i | 766 | $As_4O_x$ (m) |
| 788 | | | i | i | i | 751 | $As_4O_x$ (m) |
| 770 | | i | i | i | i | 733 | $As_4O_x$ (m) |
| 757 | | i | i | i | i | 720 | $As_4O_x$ (m) |
| 749 | i | i | i | i | i | 711 | $As_4O_x$ (m) |
| 724 | i | i | i | d | d | 682 | $As_4O_x$ |
| 712 | | | i | i | c | 676 | $As_4O_x$ |
| 590.3 | i | i | i | c | c | 561.7 | $As_4O$ (**2**) |
| 565.4 | i | i | i | c | c | 538.7 | $As_4O$ (**2**) |
| 553 | | i | i | i | i | 528 | $As_4O_x$ |
| 543 | | | | i | i | | $As_4O_x$ |
| 534 | | | | i | i | 506 | $As_4O_x$ |
| 522 | | i | i | i | i | | $As_4O_x$ |
| 498 | i | i | i | i | i | 475 | $As_4O_6$ |
| 467 | i | i | i | i | d | | ? |
| 376 | i | i | i | i | i | 363 | $As_4O_6$ |
| 324.3 | i | i | i | i | i | 324.2 | $As_4O_x$ |
| 301.5 | i | i | i | c | c | 291.0 | $As_4O$ (**2**) |
| 261 | d | d | d | d | d | 261 | $As_4$ |
| 240.5 | i | i | i | c | c | 239.3 | $As_4O$ (**2**) |

[a] Changes in band absorbance on photolysis: d = decreased (or destroyed), i = increased, and c = constant; 630(I) nm is after 20 min of 630–1000-nm photolysis, and 630(II) is after a total of 71 min of 630–1000-nm irradiation. [b] Species identified with (m) showed intermediate component(s) in $^{16,18}O_3$ isotopic experiments.

## Experimental Section

The cryogenic matrix system, ozone preparation, and matrix photolysis have been described earlier for the $PH_3$ and $P_4$ systems.[8,13-15] Elemental arsenic (Aldrich, 99.9999%, pieces) was placed in a stainless-steel Knudsen cell like that developed earlier for lithium effusion.[16] Contaminant $As_4O_6$ was removed (substantially but not completely) by heating the sample to 150–200 °C and evaporating the oxide into an argon matrix. Arsenic was sublimed at 350–375 °C into the argon/ozone (100/1 and 200/1) stream and codeposited at 15 ± 2 K for 6–10 h, the samples were photolyzed with filtered mercury arc radiation, and spectra were recorded on a Perkin-Elmer 983 infrared spectrophotometer system before and after each irradiation. Carbon dioxide impurity came from the heater element and/or the arsenic sample and decreased in successive experiments. Water contamination was minimal. No new absorptions were observed above 1000 $cm^{-1}$ that could be due to reaction with $CO_2$ or $H_2O$ impurities. Frequency accuracy is ±0.1 or ±1 $cm^{-1}$ depending on the last significant figure reported. An aluminum foil cover over the refrigerator cylinder and radiation shield made removing excess arsenic after each experiment more efficient.

## Results

After suitable preheating to remove $As_4O_6$, the vapor effusing from solid arsenic at 350–375 °C was codeposited for 10 h with argon at 14–17 K. The infrared spectrum revealed a strong, sharp 261-$cm^{-1}$ band ($A$ = absorbance = 1.0, fwhm = 6 $cm^{-1}$), a weak 204-$cm^{-1}$ band ($A$ = 0.1), and a sharp, weaker 352-$cm^{-1}$ band ($A$ = 0.02), in addition to $As_4O_6$ impurity absorptions at 831, 498, and 376 $cm^{-1}$. The former bands are due to the $\nu_3(t_2)$, $\nu_2(e)$ and $\nu_1(a_1)$ modes of the $As_4$ tetrahedron, respectively, based on agreement with the Raman spectrum of $As_4$ vapor.[11,12] The forbidden $\nu_1$ and $\nu_2$ bands were weak in the infrared spectrum presumably due to matrix site asymmetry around the large $As_4$ molecule. The allowed $\nu_3$ mode sustained a 10-$cm^{-1}$ blue shift in the matrix, demonstrating a repulsive interaction with the matrix environment. Matrix photolysis experiments with $As_4$ and $O_3$ will be described below.

**$As_4 + {}^{16}O_3$.** Infrared spectra of arsenic and ozone codeposited with argon revealed the strong $As_4$ band and ozone bands at 1104 $cm^{-1}$ ($\nu_1$, $a_1$), 704 $cm^{-1}$ ($\nu_2$, $a_1$), and 1040 $cm^{-1}$ ($\nu_3$, $b_1$).[13] The higher ozone bands exhibited new shoulders at 1096 and 1034 $cm^{-1}$. Figure 1a illustrates the spectrum from 1000 to 200 $cm^{-1}$; this spectrum also reveals sharp 921.7-, 590.3-, and 565.4-$cm^{-1}$ bands (labeled **1** and **2**) in addition to $As_4O_6$ (labeled ×) and $CO_2$ impurities. Over the course of five photolysis experiments, it was found that irradiation at 750–1000 nm decreased the 921.7-$cm^{-1}$ absorption and increased the 590.3- and 565.4-$cm^{-1}$ bands and that prolonged photolysis at 630–1000 nm in 10–20-min intervals, with high-resolution spectra recorded between each photolysis, maximized the 921.7-$cm^{-1}$ band after 20 min, while the 590.3- and 565.4-$cm^{-1}$ bands continued to increase. The spectrum after 630–1000-nm photolysis for 20 min is shown in Figure 1b; in addition to the above strong bands, weak new bands were observed at 981.5 (labeled **3**), 952.0 (labeled **4**), 770, 757, 749, 724 (labeled **5**), 553, 324.3, and 240.5 $cm^{-1}$ (labeled **2**), and the ozone satellite features were decreased. The new bands are listed in Table I. Continued 630–1000-nm irradiation for 51 min more halved the 921.7-$cm^{-1}$ band, decreased $As_4$ by 10%, doubled the 324.3-$cm^{-1}$ absorption, and increased the other new bands by 50%. Figure 1c illustrates the spectrum after 470–1000-nm irradiation for 15 min; note destruction of the 921.7-$cm^{-1}$ band, a slight increase in the other product bands, and resolution of a new feature at 712 $cm^{-1}$. Irradiation at 380–1000 nm for 30 min increased the 981.5-$cm^{-1}$ band, decreased the 952.0-$cm^{-1}$ band, produced a 961-$cm^{-1}$ band, increased 749-, 770-, 788-, and 805-$cm^{-1}$ and 553-, 543-, 534-, 522-, and 324.3-$cm^{-1}$ bands, and left the 724-, 712-, 590.3-, 565.4-, and 240.5-$cm^{-1}$ bands unchanged. Figure 1d shows the effect of 290–1000-nm radiation, which is appearance of a weak 961-$cm^{-1}$ band, continued development of the 749–804- and 553–522-$cm^{-1}$ region, increase of the $As_4O_6$ bands, slight decrease in 724- and 712-$cm^{-1}$ absorptions, and no change for the 590.3-, 565.4-, and 240.5-$cm^{-1}$ bands.

Sample annealing to 36 K after photolysis in one experiment reduced all bands slightly without altering the relative intensities

(9) Morino, Y.; Ukaji, T.; Ito, T. *Bull. Chem. Soc. Jpn.* **1966**, *39*, 64.
(10) Capwell, R. J.; Rosenblatt, G. *J. Mol. Spectrosc.* **1970**, *33*, 525.
(11) Bosworth, Y. M.; Clark, R. J. H.; Rippon, D. M. *J. Mol. Spectrosc.* **1973**, *46*, 240.
(12) Boyle, M. E. Ph.D. Thesis, University of Virginia, Charlottesville, 1987.
(13) Andrews, L.; Spiker, R. C., Jr. *J. Phys. Chem.* **1972**, *76*, 3208.
(14) Withnall, R.; Andrews, L. *J. Phys. Chem.* **1987**, *91*, 784.
(15) Withnall, R.; Andrews, L. *J. Phys. Chem.* **1988**, *92*, 4610.
(16) Andrews, L. *J. Chem. Phys.* **1969**, *50*, 4288. Experiments with arsenic powder gave more oxide impurity.

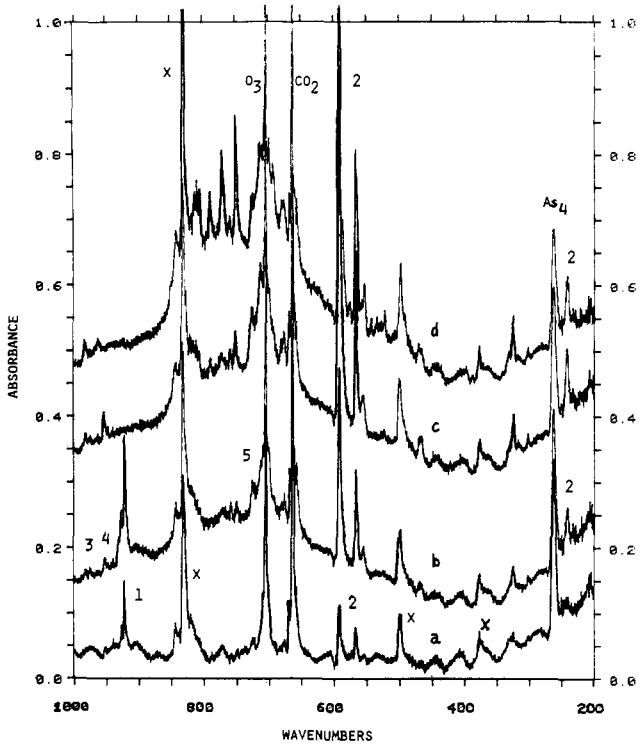


**Figure 1.** Infrared spectra of $As_4$ and $O_3$ sample from 1000 to 200 $cm^{-1}$: (a) after codeposition of $As_4$ with $Ar/O_3$ = 100/1 sample for 7 h; (b) after 630–1000-nm photolysis for 20 min; (c) after 630–1000-nm photolysis (for 51 more min) *and* 470–1000-nm photolysis (15 min); (d) after 380–1000-nm (30 min) and 290–1000-nm (20 min) photolysis.

of the 590- and 565-$cm^{-1}$ bands. One experiment was done in solid $N_2$; photolysis produced weak $N_2O$ bands, and the product spectrum was essentially unchanged from that in the argon matrix studies. In particular, the two 590- and 565-$cm^{-1}$ bands were observed with relative intensities similar to those in Figure 1.

One experiment was performed with the beam blocked during sample deposition and a germanium-coated filter in the infrared beam to prevent visible radiation from reaching the sample during the recording of the spectrum. The 921.7-, 590.3-, and 565.4-$cm^{-1}$ bands were detected in the spectrum with about half of their absorbance in Figure 1a. The Ge filter was removed, and the spectrum revealed the above bands with twice the absorbance, which were comparable to those in Figure 1a. Clearly some $As_4$–$O_3$ reaction does occur during sample condensation *in the absence of visible light*, and *visible radiation from the Nernst glower is probably responsible for some of the initial photochemistry*. A subsequent 15-min irradiation at 630–1000 nm gave the photochemical growth described above.

Two experiments were performed by evaporating $As_4$ in a quartz tube into argon passing through an open high-power microwave discharge[15] and codepositing this stream of partially decomposed arsenic vapor with an $Ar/O_3$ sample giving a final dilution greater than 300/1. Several differences were noted in the spectra as compared to Figure 1d; the $CO_2$ impurity was reduced substantially. Strong new bands were observed at 999.2 and 957.7 $cm^{-1}$; annealing decreased these bands and increased weaker bands at 995.0 and 952.4 $cm^{-1}$. Sharp 749- and 757-$cm^{-1}$ bands were prominent, and weaker 724- and 712-$cm^{-1}$ bands were resolved from the 704-$cm^{-1}$ ozone band. The 921.7-$cm^{-1}$ band was very weak, the 590- and 565-$cm^{-1}$ bands were strong, and the 261-$cm^{-1}$ $As_4$ band was about half the intensity of that from previous experiments.

Two experiments were performed with arsenic and oxygen. In the first, $As_4$ was codeposited with an $Ar/O_2$ = 100/1 sample for 6 h, and the sample was photolysed with 630-, 470-, and 220–1000-nm radiation; no product bands appeared. In the second, $As_4$ was codeposited with an $Ar/O_2$ = 50/1 stream passed through a *low-power* open microwave discharge[15] for 4 h where radiation from the discharge makes minimal contribution. A weak $O_3$ band

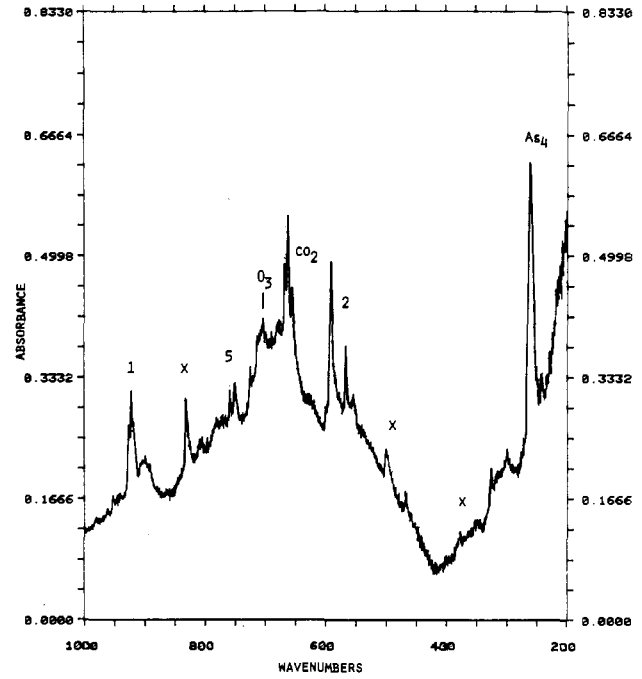


**Figure 2.** Infrared spectrum from 1000 to 200 $cm^{-1}$ of $As_4$ codeposited with $Ar/O_2$ = 50/1 stream passed through a low-power microwave discharge for 4 h.

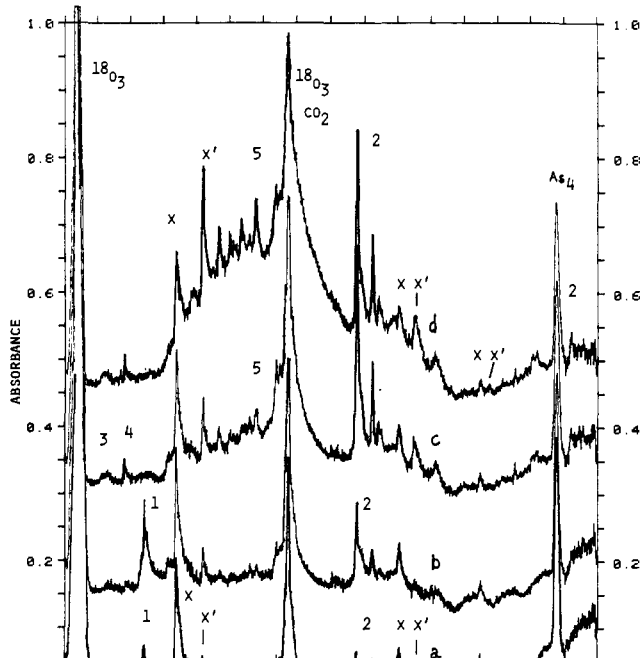


**Figure 3.** Infrared spectra of $As_4$ and $^{18}O_3$ sample: (a) after codeposition of $As_4$ with $Ar/^{18}O_3$ = 100/1 for 5 h; (b) after 630–1000-nm photolysis (15 min); (c) after 470–1000-nm photolysis (22 min); (d) after 380–1000-nm (30 min) and 290–1000-nm (20 min) photolysis.

was observed at 1040 $cm^{-1}$ without any 1034-$cm^{-1}$ absorption. The spectrum shown in Figure 2 reveals many of the same product bands observed on 630–1000-nm photolysis (Figure 1b) and demonstrates that the net effect of the matrix chemistry performed here is *oxygen atom* transfer to $As_4$. Continued codeposition with high-power discharge for 2 h decreased the 921.7-$cm^{-1}$ band and increased all other absorptions, analogous to the effect of photolysis in Figure 1.

**$As_4$ + $^{18}O_3$.** Three experiments were done with $^{18}O_3$ and $As_4$, and the spectra, with appropriate oxygen isotopic shifts, are very similar to those presented for normal isotopic ozone. Figure 3

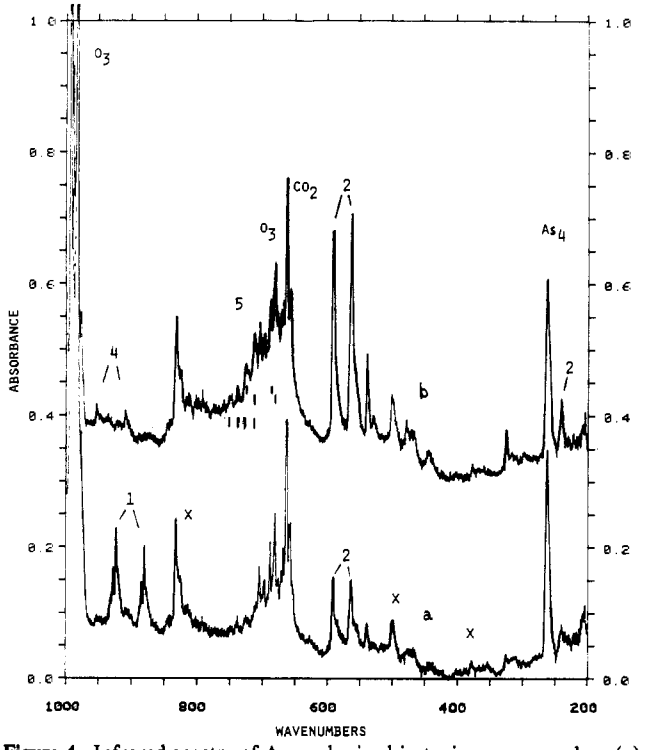


**Figure 4.** Infrared spectra of $As_4$ and mixed-isotopic ozone samples: (a) after 630–1000-nm photolysis; (b) after 470–1000-nm photolysis.

illustrates the analogous photolysis spectra, and Table I lists the isotopic product bands; the first product bands shifted to 878.8, 561.7 and 538.7 $cm^{-1}$. Note in Figure 3a the presence of a new 790.5-$cm^{-1}$ band (labeled ×′), which is obviously the oxygen-18 counterpart of the 831-$cm^{-1}$ $As_4O_6$ impurity band, and the growth of this 790.5-$cm^{-1}$ band during the photolysis sequence. The weaker $As_4O_6$ impurity bands at 498 and 376 $cm^{-1}$ also acquired oxygen-18 counterparts at 475 and 363 $cm^{-1}$. One experiment was done with more dilute ozone ($Ar/^{18}O_3$ = 200/1), and there appeared to be no concentration effects other than a reduction in product absorbances. Even in this experiment, the 878.8- and 790.5-$cm^{-1}$ bands were detected in the original sample. As before, 630-nm photolysis increased the 878.8-$cm^{-1}$ absorption and produced the 682-, 676-, 561.7-, and 538.7-$cm^{-1}$ bands, and 420-nm irradiation destroyed the 878.8-$cm^{-1}$ band, increased the above bands, and produced weak new bands at 766, 751, 720, and 711 $cm^{-1}$.

**$As_4$ + $^{16,18}O_3$.** Two analogous experiments were done with arsenic and mixed-isotopic ozone, and the infrared spectra were for the most part a superposition of Figures 1 and 3. Spectra after 630- and 470-nm photolysis are shown in Figure 4. Notice the sharp doublets in Figure 4a at 921.7 and 878.8 $cm^{-1}$ and at 590.3 and 561.7 $cm^{-1}$ and the sharp 538.7-$cm^{-1}$ band whose oxygen-16 counterpart (at 565.4 $cm^{-1}$) is covered by the stronger 561.7-$cm^{-1}$ band. Figure 4b shows destruction of the 921.7- and 878.8-$cm^{-1}$ doublet, growth of the sharp 952.0- and 908.0-$cm^{-1}$ doublet and further growth of the 590.3-, 561.7-, and 538.7-$cm^{-1}$ bands. In the 830–710-$cm^{-1}$ region below $As_4O_6$, however, many new intermediate mixed-isotope components were observed on 290-nm photolysis. Owing to overlapping of bands, it is not possible to uniquely assign mixed-isotopic bands to a particular pair of $^{16}O_3$ and $^{18}O_3$ counterparts listed in Table I, but it is clear that mixed-isotopic species are present for the bands noted (m) in the table.

In the 710–660-$cm^{-1}$ region, overlapping with $^{16,18}O_3$ bands presented another complication; however, *product bands increase and isotopic ozone bands decrease* on photolysis. Intermediate components were not observed for the 724- and 712-$cm^{-1}$ bands, which broadened, and the 749-$cm^{-1}$ band aquired new mixed-isotopic components at 738 and 778 $cm^{-1}$.

**$As_4O_6$ + Ozone.** Similar photolysis experiments were done for $As_4O_6$ vapor codeposited with each isotopic ozone sample primarily to insure that none of the above product absorptions were due to reaction of oxygen atoms with an $As_4O_6$ impurity. Irradiation of $^{16}O_3$ samples at 630–1000 nm gave no products, in contrast to $As_4$ experiments. Photolysis at 420–1000 nm gave new bands at 1019, 850, 844, 584, 567, 544.0, 509, 393, and 370 $cm^{-1}$. These bands increased on 220–1000-nm photolysis, and new bands appeared at 1032, 1025, 861.2, 584.8, 567, 530, and 386 $cm^{-1}$. Photolysis of $^{16,18}O_3$ samples gave a new 974-$cm^{-1}$ band and the above product bands unshifted in position. Irradiation of $^{18}O_3$ samples again gave the same product bands (970–1000-$cm^{-1}$ region obscured by $^{18}O_3$) except for small shifts to 860.7, 584.1, and 543.6 $cm^{-1}$. *None of the new product bands in $As_4$ experiments were observed in the $As_4O_6$ studies.* Comparison with earlier matrix studies[7] of $As_4O_7$, $As_4O_8$, and $As_4O_9$ shows good agreement with the above bands. The 490–590-$cm^{-1}$ region in the present spectrum is particularly diagnostic and similar to the earlier report. On 420–1000-nm photolysis, bands due to $As_4O_7$ and $As_4O_8$ were produced; these grew on 220–1000-nm photolysis while bands due to $As_4O_9$ appeared in the spectrum.

## Discussion

The new species produced by elemental arsenic reactions with ozone will be identified. Several benchmark frequencies will be used for this identification: (a) the AsO diatomic fundamental is 956.6 $cm^{-1}$ in the gas phase,[2] which is the region expected for terminal "As=O" vibrations, and (b) the 831- and 498-$cm^{-1}$ absorptions for $As_4O_6$ are due to antisymmetric phasing of antisymmetric and symmetric As–O–As single bond vibrations, respectively.[3-5]

A major question in understanding the reaction of $As_4$ with $O_3$ or O atoms is the possible stabilization of $As_4O$ before it can decompose to $As_2$ and $As_2O$ or $As_3$ and AsO. Since the AsO bond energy is approximately 115 kcal/mol and the dissociation energy of $As_4$ to $2As_2$ is 72 kcal/mol,[17] it is possible for the initially formed energetic $[As_4O]^*$ species to eliminate $As_2$ and form $As_2O$ before relaxation by the matrix. Furthermore, on the basis of the heat of formation of $As_3$ (57.6 kcal/mol),[18] the reaction $As_4 + O \rightarrow As_3 + AsO$ is exothermic (−18.6 kcal/mol) and must also be considered in the matrix system. Clearly diatomic AsO species can be recognized from their characteristic isotopic shift. However, the straightforward way to identify possible $As_2O$ products is to compare matrix reactions of $As_4$ and $As_2$ with $O_3$. A series of experiments with ozone and $As_2$ effusing from heated GaAs gave sharp, strong 999.6-, 957.7-, 952.4-, 847.1-, and 787.1-$cm^{-1}$ bands.[19] No absorptions were observed at 921.7, 590.3, and 565.4 $cm^{-1}$, which are the major products of the $As_4 + O_3$ photolysis reactions described in this paper. Clearly, the latter are due to $As_4$ reaction products, and the former are due to $As_2$ reaction products. The $As_2$ reaction with isotopic ozones will be described in detail later,[19] but it is important to note here that the 999.6- and 957.7-$cm^{-1}$ bands exhibited mixed isotopic doublets and AsO diatomic $^{18}O$ shifts. The latter is obviously due to isolated AsO, and the former is most probably linear $As_2O$, which was not detected in the present $As_4 + O_3$ photochemical reactions. Hence, the failure to observe major $As_2 + O_3$ products in the $As_4 + O_3$ reaction indicates that the major products in the latter reaction retain the $As_4$ stoichiometry within the matrix cage.

**AsO.** The sharp, weak 952.0-$cm^{-1}$ band (labeled 4) increased with 630- and 470-nm photolysis and was replaced with a 961-$cm^{-1}$ band on near-UV photolysis. Both bands exhibited $^{18}O$ counterparts appropriate for a diatomic molecule, and the doublet in Figure 4b characterizes the vibration of a single oxygen atom. Near agreement with the gas-phase fundamental and between the calculated (44.7 $cm^{-1}$), and observed (44.0 $cm^{-1}$) oxygen-18 shifts suggest assignment of the 961- and 952-$cm^{-1}$ bands to perturbed AsO in solid argon. Further support is found in the proximity of the strongest arsine oxide ($H_3AsO$) absorption[20] at 938 $cm^{-1}$

(17) Wagman, D. D.; et al. *J. Phys. Chem. Ref. Data Suppl. 2* **1982**, *11*.
(18) Bennett, S. L.; Margrave, J. L.; Franklin, J. L.; Hudson, J. E. *J. Chem. Phys.* **1973**, *59*, 5814.
(19) McCluskey, M.; Andrews, L. To be submitted for publication.
(20) Andrews, L.; Withnall, R.; Moores, B. *J. Phys. Chem.* **1989**, *93*, 1279.

and the similar proximity of phosphine oxide and PO diatomic absorptions at 1240 and 1218 $cm^{-1}$, respectively.[14] The decrease of one perturbed AsO species and growth of the other with ultraviolet photolysis may be due to reorientation with the other arsenic byproduct in the matrix cage. Molecular $As_4$ passed through a microwave discharge and codeposited with $O_3$ in excess argon gave a sharp 957.7-$cm^{-1}$ band, which is probably due to isolated AsO in solid argon. Annealing decreased the 957.7-$cm^{-1}$ band and increased the 952-$cm^{-1}$ band assigned to AsO···X, where X is probably an arsenic atom.

**Species 1, 2, and 3.** The major product in the early stages of sample photolysis was the sharp 921.7-$cm^{-1}$ feature, and in the later stages, the strong 590.3- and 565.4-$cm^{-1}$ doublet dominated and a weaker 981.5-$cm^{-1}$ band appeared. Figure 4a demonstrates that the strong absorptions are due to single oxygen atom vibrations. The scrambled isotopic ozone experiment also revealed the $^{18}O$ counterpart for the 981.5-$cm^{-1}$ band at 935.5 $cm^{-1}$ and no intermediate mixed counterpart although $^{18}O_3$ absorption masked the 981.5-$cm^{-1}$ band. The photochemical observations strongly suggest that species **1** and **2** have a common stoichiometry; in particular 750–1000-nm irradiation of a sample with the 921.7-, 590.3-, and 565.4-$cm^{-1}$ bands only decreased the 921.7-$cm^{-1}$ band and increased the 590.3- and 565.4-$cm^{-1}$ absorptions.

The analogous $P_4 + O_3$ reaction gave terminal and bridged $P_4O$ and perturbed PO species as major products; terminal $P_4O$ appeared on red photolysis and was stable to UV photolysis that produced a low yield of bridged $P_4O$; perturbed PO species increased and decreased throughout the photolysis sequence. Obvious differences between the $P_4$ and $As_4$ ozone systems are apparent; the major product $P_4O$ appeared first and dominated throughout the photolysis sequence, but the major initial $As_4$ product at 921.7 $cm^{-1}$ was destroyed by visible radiation and weaker bands at 981.5 and 952.0 $cm^{-1}$ were produced. These absorptions involve a single oxygen atom. Which one (if any) of these bands can be assigned to the expected terminal $As_4O$ species? Growth on visible photolysis, stability to ultraviolet photolysis, and frequency relative to AsO suggest 981.5 $cm^{-1}$, but initial band yield suggests 921.7 $cm^{-1}$. Although we cannot be absolutely certain, photolysis behavior is probably a better criterion than yield, and on this basis, the 981.5-$cm^{-1}$ band is assigned to terminal $As_4O$ (**3**) and the 921.7-$cm^{-1}$ band is attributed to the photosensitive $(As_3)(AsO)$ complex (**1**). The growth of $As_4O_x$ ($x$ = 6–9) and $H_3AsO$ on ultraviolet and visible photolysis in these and earlier experiments[20] further suggests that terminal $As_4O$ should also grow and be stable on photolysis. Isotopic shifts are in accord with this chioce; both bands exhibited almost pure AsO diatomic $^{18}O$ shifts (calculated 878.5 $cm^{-1}$, observed 878.8 $cm^{-1}$; calculated 935.4 $cm^{-1}$, observed 935.5 $cm^{-1}$). The photosensitive $(As_3)(AsO)$ complex can yield other perturbed AsO species (**4**) discussed above and the bridge-bonded $As_4O$ isomer (**2**) to be discussed next. Species **4** is most likely As···AsO, which exhibits a smaller perturbation than $(AsO)(As_3)$ where oxygen may interact with three arsenic atoms.

The 590.3- and 565.4-$cm^{-1}$ bands maintained approximately constant relative intensities upon ozone photolysis *and* upon discharge O atom reactions, which suggests a common stoichiometry. The 590.3-$cm^{-1}$ band exhibited a lower oxygen-18 fundamental (561.7 $cm^{-1}$) than that calculated (562.6 $cm^{-1}$) for a diatomic As–O oscillator, which is in accord with an antisymmetric As–O–As stretching mode. This group can be formed by bonding oxygen to one edge of tetrahedral $As_4$. Using the edge dimension (2.43 Å)[21] and the As–O bond length in $As_4O_6$ (1.78 Å)[22] gives an apex angle of 86°. If this edge dimension were increased to 2.77 Å, the apex angle would be 102°, in agreement with that predicted from the $^{18}O$ shift by assuming a pure antisymmetric As–O–As stretching mode. In $As_4O_6$, the As–As distances and As–O–As angles are further increased to 3.20 Å and 128°, respectively, as the edges of the $As_4$ tetrahedron are replaced by bridging oxygen atoms. Therefore, a bridged $As_4O$ cage is a reasonable source for the 590.3-$cm^{-1}$ band. The associated 240.5-$cm^{-1}$ band is assigned to a largely As–As stretching mode in the $As_4O$ cage, and the weak 301.5-$cm^{-1}$ band is appropriate for a symmetric As–O–As stretching mode. An alternative five-membered ring $As_4O$ structure could also account for the bridged As–O–As vibrations. Finally, the 565.4-$cm^{-1}$ band is best assigned to a bridged $As_4O$ species with a different matrix perturbation or structure.

**Scheme I.** Mechanism

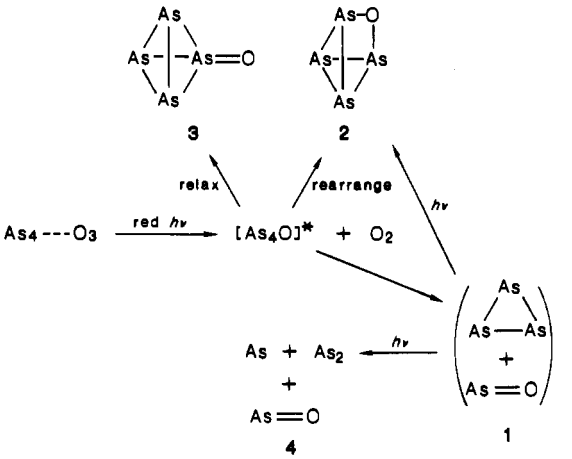


**Higher Bridged Species.** The product bands between 712 and 831 $cm^{-1}$ exhibit a photochemical evolution following the species **1** and **2** bands and beginning with 630-nm radiation producing the 712- and 724-$cm^{-1}$ bands and ending with the 831-$cm^{-1}$ $As_4O_6$ band growing on 290-nm photolysis. The proximity of the new bands to the strongest infrared absorption of $As_4O_6$ at 831 $cm^{-1}$ and the growth of $As_4O_6$ itself with short-wavelength photolysis provide evidence for identification of these products as bridge-bonded $As_4O_x$ cage species. In mixed $^{16,18}O_3$ isotopic experiments, the 724- and 712-$cm^{-1}$ bands broadened and intermediate components were not observed. The 749- and 711-$cm^{-1}$ bands for $^{16}O$ and $^{18}O$, respectively, exhibited intermediate components at 738 and 728 $cm^{-1}$, which is appropriate for the most stable $As_4O_3$ species. The 770-, 788-, and 805-$cm^{-1}$ bands exhibit additional multiplet components and are probably due to higher $As_4O_x$ species. The weak 324.3-$cm^{-1}$ band is probably due to one of these species. Although the photochemical production of $As_4O_6$ in these experiments may be surprising (the $As_4O_6$ bands doubled during the photochemistry of Figure 1), this observation is confirmed by the appearance of $As_4{}^{18}O_6$ in the $^{18}O_3$ experiments. It is postulated that $As_4O_6$ is formed in these experiments from the photochemical reaction of $As_4$ and two ozone molecules in the same matrix cage.

**$As_4$---$O_3$.** The shoulder absorptions at 1034 and 977 $cm^{-1}$ on $^{16}O_3$ and $^{18}O_3$ bands at 1040 and 982 $cm^{-1}$, respectively, and at 1096 and 1035 $cm^{-1}$ on 1104- and 1042-$cm^{-1}$ isotopic ozone fundamentals are assigned to the $As_4$---$O_3$ complex. The important observation is that the complex bands were destroyed by the 630–1000-nm radiation that produced first species **1** and **2** and next species **3** and **4**. It is thus immediately obvious that the photochemistry of the ozone submolecule has been altered in the complex with $As_4$. Normally ozone absorption in the red is very weak,[23] and matrix photolysis of isolated ozone at 630–1000 nm causes a *minimal* decrease in the ozone infrared fundamentals. However, specific interaction with arsenic in the complex markedly increased the photodissociation probability of ozone with red radiation; oxygen atom transfer produced an energized $[As_4O]^*$ species that relaxed to give $As_4O$ and predominantly other species.

$$As_4\text{---}O_3 \xrightarrow{\text{red } h\nu} [As_4O]^* + O_2$$

The $As_4$---$O_3$ complex appears to be stronger than its $P_4$ and $PH_3$ counterparts based on the shifts in ozone fundamentals in each complex,[8,24] $\Delta\nu_3$ = 2.7 and $\Delta\nu_1$ = 2.0 $cm^{-1}$ for $PH_3$---$O_3$ and $\Delta\nu_3$

(21) Morino, Y.; Ukaji, T.; Ito, T. *Bull. Chem. Soc. Jpn.* **1966**, *39*, 64.
(22) Wilson, A. J. C., Ed. *Struct. Rep.* **1955**, *9*, 293.
(23) Griggs, M. *J. Chem. Phys.* **1968**, *49*, 857.

= 6, $\Delta\nu_1$ = 4 $cm^{-1}$ for $P_4$--$O_3$ compared to $\Delta\nu_3$ = 6 and $\Delta\nu_1$ = 8 $cm^{-1}$ for $As_4$--$O_3$. This interaction between submolecules in the complex is responsible for the photochemistry and the resulting O atom transfer.

**Mechanism.** The proposed photochemical reaction mechanism (Scheme I) begins with the $As_4$---$O_3$ complex described above. The $[As_4O]^*$ product species is initially excited by the energy of the new terminal "As=O" bond, which can be approximated by the AsO diatomic thermochemical value (115 kcal/mol). This means that matrix relaxation of $[As_4O]^*$ must occur straight away or rearrangement and decomposition may occur. Only a small yield of terminal $As_4O$ is trapped here. The formation of AsO directly from $[As_4O]^*$ requires that the As byproduct be bound to $As_2$ to give an $As_3$ species; otherwise, the reaction of $As_4$ + O to give AsO + As + $As_2$ is endoergic by 49 kcal/mol. In fact $[As_4]O^*$ can decompose directly to $As_3$ and AsO in the same matrix cage, and this $(As_3)(AsO)$ complex is expected to photolyze to give other AsO species and bridged $As_4O$.

Bridged $As_4O$ (**2**) can be formed directly by rearrangement of $[As_4O]^*$ during relaxation in the initial photochemical step or upon the insertion of $O(^1D)$ into an As-As bond in $As_4$ in the UV photolysis studies. After one bridged oxygen is affixed to $As_4$, others can be added, leading to the formation of $As_4O_6$. Although specific $As_4O_x$ ($x$ = 2-5) species cannot be identified with certainty, it is clear that stepwise addition of oxygen atoms to $As_4$ occurs, leading finally to the stable species $As_4O_6$. Support for this mechanism is found in mass spectroscopic evidence for $As_4O_3$, $As_4O_4$, and $As_4O_5$.[25] In addition it is believed that the $As_4$---$O_3$ complex can also give $As_4O_3$ on photolysis and that two ozone molecules trapped in the same matrix site with $As_4$ can also give $As_4O_6$ on photolysis. Note that the reaction of $As_4$ and $O_3$ occurs on sample preparation as evidenced by $As_4{}^{18}O_6$ in the initial sample deposit for $As_4$ and $^{18}O_3$.

Finally, the observation of weak bands for species **1** and **2** in a sample exposed only to the infrared examining radiation means that some $As_4$ and $O_3$ react spontaneously under the deposition conditions. The analogous reaction of $As_4$ and $O_2$ was not observed, but O atoms gave the same $As_4$ reaction products as ozone. The present observations attest to the great reactivity for $As_4$ with ozone.

## Conclusions

The codeposition of $As_4$ and $O_3$ with excess argon at a low temperature produced sharp weak bands at 921.7 and 590.3 $cm^{-1}$. Red-light photolysis first increased the former more than the latter, but prolonged red-light photolysis decreased the former, increased the latter and produced a 565.4-$cm^{-1}$ satellite, and formed a 952.0-$cm^{-1}$ band. Scrambled isotopic ozone experiments revealed isotopic doublets for these bands, which is characteristic of the vibration of a single oxygen atom. Although it is difficult to be certain about the arsenic stoichiometry and structure, these single O atom species are believed to be due to $(As_3)(AsO)$ complex, bridge-bonded $As_4O$, and perturbed AsO product species, respectively. Continued photolysis with visible and near-ultraviolet light produced a weak new band at 981.5 $cm^{-1}$ and new bands in the 712-805-$cm^{-1}$ region approaching that of $As_4O_6$. The latter are assigned to bridge-bonded $As_4O_x$ cage species ($x$ = 2-5). On the basis of comparison with the $P_4$ + O system, the 981.5-$cm^{-1}$ band is probably due to the terminally bonded $As_4O$ species. The excited $[As_4O]^*$ species produced in the initial reaction is not relaxed as efficiently by the matrix as $[P_4O]^*$, and decomposition and rearrangement products formed and trapped in the matrix cage dominate in the matrix spectra. Finally, $As_4$ is more reactive with $O_3$ than $P_4$ in matrix codeposition experiments.

**Acknowledgment.** We gratefully acknowledge financial support from NSF Grant CHE85-16611 and guidance from the first $As_4$ experiments performed by M. E. Boyle and R. Withnall.

**Registry No.** **1**, 118576-12-8; **2**, 118576-13-9; **3**, 118576-14-0; **4**, 12005-99-1; **5**, 118576-15-1; $As_4$, 12187-08-5; $O_3$, 10028-15-6; $^{18}O$, 14797-71-8.

(24) Withnall, R.; Hawkins, M.; Andrews, L. *J. Phys. Chem.* **1986**, *90*, 575.
(25) Brittain, R. D.; Lau, K. H.; Hildenbrand, D. L. *J. Phys. Chem.* **1982**, *86*, 5072.

Contribution from the Department of Chemistry, University of Minnesota, Minneapolis, Minnesota 55455

# UV-Vis-IR Thin-Layer Spectroelectrochemical Studies of Hexakis(aryl isocyanide)chromium Complexes. In Situ Generation and Characterization of Four Oxidation States

John P. Bullock and Kent R. Mann*

*Received March 30, 1989*

Spectroelectrochemistry in the UV-vis and IR spectral regions has been used to characterize the Cr(0), Cr(I), Cr(II), and Cr(III) analogues of a series of chromium hexakis(aryl isocyanide) complexes. Controlled-potential bulk electrolyses in an improved thin-layer spectroelectrochemical cell were monitored with UV-vis and FT-IR spectrometers in separate experiments. All electrolyses proceeded isosbestically and were chemically reversible. IR data show that each sequential oxidation results in higher $\nu_{CN}$ stretching frequencies and lower absolute integrated intensities for the $\nu_{CN}$ absorption. This is related to the decrease in $d\pi-\pi^*_{CN}$ back-bonding in the more oxidized forms. Rough correlations between the electron-releasing ability of the aryl substituent and both the $\nu_{CN}$ stretching frequency and the absolute integrated intensities of the Cr(III) complexes are observed. This is attributed to varying degrees of $\sigma_{CNR} \rightarrow$ Cr donation, which become apparent only when the degree of $d\pi-\pi^*_{CN}$ back-bonding is small. UV-vis experiments show that for all compounds studied the ligand-to-metal charge-transfer (LMCT) band energy decreases upon successive oxidation, while the energy of the MLCT band increases. This is in accord with the increased oxidation strength of the central chromium ion. A correlation can also be made between the electron-releasing abilities of the aryl substituents and the energies of the LMCT electronic transitions in the Cr(II) and the Cr(III) complexes. This reflects the greater $\sigma_{CNR} \rightarrow$ Cr donation of aryl isocyanides with electron-donating substituents and is consistent with the trend in the absolute integrated intensities of Cr(III) species observed in IR experiments.

## Introduction

The electrochemistry of hexakis(aryl isocyanide)chromium complexes has been studied by several groups in recent years.[1-6] These compounds undergo a series of reversible one-electron-transfer reactions at solid electrodes, resulting in formal chromium

* To whom correspondence should be addressed.

(1) Treichel, P. M.; Dirreen, G. E. *J. Organomet. Chem.* **1972**, *39*, C20.
(2) Treichel, P. M.; Essenmacher, G. J. *Inorg. Chem.* **1976**, *15*, 146.
(3) Essenmacher, G. J.; Treichel, P. M. *Inorg. Chem.* **1977**, *16*, 800.

0020-1669/89/1328-4006$01.50/0 